Author Manuscript
Author Manuscript
Author Manuscript
Author Manuscript

HHS Public Access
Author manuscript
Semin Nucl Med. Author manuscript; available in PMC 2023 May 01.

Published in final edited form as:
Semin Nucl Med. 2022 May ; 52(3): 330–339. doi:10.1053/j.semnuclmed.2022.01.002.

Total-body PET/CT – first clinical experiences and future perspectives

Quinn Ng, MD, PhD[1], **Elizabeth Katherine Anna Triumbari, MD**[1,2], **Negar Omidvari, PhD**[3], **Simon R. Cherry, PhD**[1,3], **Ramsey D. Badawi, PhD**[1,3], **Lorenzo Nardo, MD, PhD**[1]

[1]Department of Radiology, UC Davis, Sacramento, CA, USA

[2]Section of Nuclear Medicine, University Department of Radiological Sciences and Hematology, Università Cattolica del Sacro Cuore, Rome, Italy

[3]Department of Biomedical Engineering California Davis, CA, USA

Abstract

Total-body PET has come a long way from its first conception to today, with both total-body and long axial field of view (> 1m) scanners now being commercially available world-wide. The conspicuous signal collection efficiency gain, coupled with high spatial resolution, allows for higher sensitivity and improved lesion detection, enhancing several clinical applications not readily available to current conventional PET/CT scanners. This technology can provide (a) *reduction in acquisition times* with preservation of diagnostic quality images, benefitting specific clinical situations (i.e. pediatric patients) and the use of several existing radiotracers that present transient uptake over time and where small differences in acquisition time can greatly impact interpretation of images; (b) *reduction in administered activity* with minimal impact on image noise, thus reducing effective dose to the patient, improving staff safety, and helping with logistical concerns for short-life and poor dosimetry profiled radiotracers that have had limited use on conventional PET scanners until now; (c) *delayed scanning*, that has shown to increase the detection of even small and previously occult malignant lesions by improved clearance in regions of significant background activity and by reduced visibility of coexisting inflammatory processes; (d) *improvement in image quality*, as a consequence of higher spatial resolution and sensitivity of total-body scanners, implying better appreciation of small structures and clinical implications with downstream prognostic consequences for patients; (e) *simultaneous total-body dynamic imaging*, that allows the measurement of full spatiotemporal distribution of radiotracers, kinetic modeling, and creation of multiparametric images, providing physiologic and biologically relevant data of the entire body at the same time.

Corresponding Author: Lorenzo Nardo, **Address:** 4860 Y street suite 3100, Telephone number: 001 916 734 2754, lnardo@ucdavis.edu.

Authors' declaration of interest +/− funding sources:
Lorenzo Nardo has is principal investigator of a service agreement with United Imaging Healthcare. UC Davis has a revenue-sharing agreement with United Imaging Healthcare that is based on uEXPLORER sales.
The authors thank all the EXPLORER team at UC Davis. The authors acknowledge NIH R01CA249422-01.

Submission declaration: The article has not been published previously, it is not under consideration for publication elsewhere, its publication is approved by all authors and tacitly or explicitly by the responsible authorities where the work was carried out, and that, if accepted, it will not be published elsewhere in the same form, in English or in any other language, including electronically without the written consent of the copyright holder.
This paper has been supported by NIH 5R01CA249422-03.

Author Manuscript Author Manuscript Author Manuscript Author Manuscript

On the other hand, the higher physical and clinical sensitivity of total-body scanners bring along some limitations. The strong impact on clinical sensitivity potentially increases the number of false positive findings if the radiologist does not recalibrate interpretation considering the new technique. Delayed scanning causes logistical issues and introduces new interpretation questions for radiologists. Data storage capacity, longer processing and reconstruction time issues are other limitations, but they may be overcome in the near future by advancements in reconstruction algorithms and computing hardware.

Keywords

Total-body PET; extended axial field-of-view; quantification; acquisition time; dynamic PET

1. Introduction

The concept of total-body positron emission tomography (PET) with an extended axial field-of-view (AFOV) was first conceptualized in technical sketches presented by Dr. Terry Jones in the early 90s, in which two flat panels of detectors covered the entire torso to offer simultaneous imaging of all major organs with increased acceptance angle. The idea of developing long AFOV PET tomograph was further explored by different research groups in several proposals, simulation studies, and efforts in developing PET scanners with an increased axial extent, particularly to study the benefits from the signal collection efficiency gain (R.D. Badawi et al., 2019; Cherry, 2006; Conti et al., 2006; Crosetto, 2003; Eriksson et al., 2007; Watanabe et al., 2004; Wong et al., 2007). The first total-body PET in the US was installed at the University of California, Davis (UC Davis) in 2019 (Nardo et al., 2021) and total-body and long AFOV (> 1m) PET scanners are now commercially available world-wide.

The uEXPLORER, developed through collaboration between UC Davis and United Imaging Healthcare (UIH) as part of the EXPLORER Consortium, is a total-body PET/CT tomograph with a transaxial field of view (FOV) of 68.6 cm and a total AFOV length of 194.0 cm (Spencer et al., 2021), compared to conventional PET scanners with AFOVs varying from 15 cm to 35 cm. The conspicuous signal collection efficiency gain coupled with high spatial resolution allows for several enhanced clinical applications not readily available to current commercial FOV scanners including: (a) reduction in acquisition times, (b) reduction in administered activity, (c) delayed scanning, (d) improvement in image quality, and (e) simultaneous total-body dynamic imaging. On the other hand, these features lead to image structures that were not seen before or were seen veiled by the partial volume effect, initially causing substantial debate with oncologists, concerned about patient care implications. In particular, the physical sensitivity (collection efficiency) of the scanner has a relationship with the increased clinical sensitivity in detecting both anatomic and pathologic small structures and characterizing/quantifying findings with higher spatial resolution and conspicuity can be challenging to explain at the beginning of the implementation of the scanner in the clinical routine. Therefore, the installation of several total-body PET/CT scanners in four different continents, including the uEXPLORER at Zhongshan Hospital, Shanghai, China (Ramsey D. Badawi et al., 2019), the PennPET EXPLORER at University

Author Manuscript Author Manuscript Author Manuscript Author Manuscript

of Pennsylvania, USA (Karp et al., 2020), the Siemens Biograph Vision Quadra at Inselspital University Hospital in Bern, Switzerland (Alberts et al., 2021) and at Royal Prince Alfred Hospital, Sydney, Australia has brought up the need of a better understanding of the capabilities of this technology.

In this work, we describe the main uEXPLORER characteristics, their impact on diagnosis and quantification of imaging findings, along with some clinical challenges encountered during the clinical implementation of the first total-body scanner. We also present future perspectives on opportunities that total-body and long AFOV PET scanners offer.

2. Scanner characteristics and impact on diagnosis and quantification

The uEXPLORER total-body PET/CT tomograph is composed of 8 PET units along the axial direction, forming the system's total axial length of 194.0 cm. Each PET unit has 24 detector modules containing 70 block-detectors. The detector blocks are made of a 5 × 7 array of 2.76 × 2.76 × 18.1 mm3 Lutetium Yttrium Oxyorthosilicate (LYSO) crystals with a 2.85 mm crystal pitch, coupled to a 4 × 4 array of 6 × 6 mm2 silicon photomultipliers (SiPMs). The PET system is integrated with an 80-row, 160-slice helical CT scanner with rotation time down to 0.5 sec and minimum slice thickness of 0.5 mm. The uEXPLORER PET scanner was characterized in a recent study, using the NEMA NU 2–2018 standard protocol and additional adapted measurements particularly designed for characterization of total-body PET scanners (Spencer et al., 2021). Sensitivity measurements with a 170 cm-long line source, representing the adult human length, showed a total signal collection sensitivity of 147 kcps/MBq at the center, which demonstrates a 15–68-fold signal collection sensitivity gain compared to commercially available conventional PET scanners at the time (Spencer et al., 2021).

In addition to the high total sensitivity, the uEXPLORER is the only total-body PET system that offers uniform sensitivity throughout its central one-meter length, using a 57° acceptance angle. Unlike the triangular shape of the sensitivity profile in other PET systems, the one-meter-long uniform sensitivity region makes it possible to simultaneously image most organs of interest in adults, in a single bed position, with uniform image quality. This has been demonstrated by a series of image quality phantom scans performed throughout the AFOV of the scanner (Spencer et al., 2021). The increased acceptance angle in the uEXPLORER raises questions, particularly on the trade-off between sensitivity, spatial resolution, and true count rate (Xuezhu Zhang et al., 2018). On the one hand, including more oblique lines-of-response (LORs) increases the sensitivity, but on the other hand these LORs are generally more prone to count losses, due to increased attenuation, resulting in increased Compton scatter fraction and increased relative random rate. Furthermore, the oblique LORs introduce larger axial parallax errors, resulting in spatial resolution degradation. However, depending on the specific imaging application, these parameters can have different overall image-quality impact and can be particularly subject size-dependent.

To understand the impact of the increased axial parallax error on spatial resolution in clinical settings, it is important to fully consider the parameters affecting the spatial resolution and subsequently lesion detection capability of the total-body PET scanner using iterative

Author Manuscript Author Manuscript Author Manuscript Author Manuscript

reconstruction methods. The high sensitivity, in addition to the use of 2.85 mm pitched LYSO crystals in the system, creates high spatial resolution capability for the uEXPLORER. This is demonstrated in the NEMA NU 2–2018 spatial resolution tests using filtered backprojection (FBP) image reconstruction with restricted acceptance angle, in which ~3 mm spatial resolution (FWHM) at 1 cm offset from the center of the FOV is achieved (Spencer et al., 2021). However, like all other commercial clinical PET scanners today, the uEXPLORER uses iterative image reconstruction algorithms for clinical imaging, and spatial resolution in such case is heavily affected by reconstruction parameters such as iteration number, source contrast, object size, point-spread-function (PSF) modelling, voxel size, interpolation, and smoothing functions. While using iterative image reconstruction can generally lead to improved spatial resolution compared to filtered back-projection, the effects of such parameters on spatial resolution can be significantly larger than the effects from the increased acceptance angle. Our current spatial resolution characterization tests with the clinical reconstruction software of the uEXPLORER suggest that the axial parallax effects on transaxial resolution are negligible, and at low-contrast settings at early iterations, less than 1 mm degradation of the axial spatial resolution can be expected in the central region of the scanner compared to the 1/16th of the AFOV that uses an acceptance angle of 17°. This difference in axial resolution is affected by iteration number and source contrast and can be mitigated to less than 0.5 mm by iterating longer, supported by the high sensitivity.

To further move from the spatial resolution capability to lesion detection capability, it is important to note that in many cases, the main limiting factor in lesion detection is the image noise and, in such cases, it is only in combination with high detection sensitivity that the high spatial resolution can lead to improved lesion detection. This is partly reflected in contrast recovery curves of the NEMA IQ phantom, in which significant improvements in contrast recovery coefficient of the two smallest spheres (10 mm and 13 mm diameter) are observed compared to other clinical systems, particularly when 10 iterations (20 subsets) are used instead of 4 iterations (20 subsets). Furthermore, comparing the background variability curves in the same case shows that the high sensitivity of the scanner allows iterating longer up to 10 iterations (20 subsets) to further improve the contrast recovery of the smallest spheres, without significant increase in image noise. As contrast recovery and detectability of larger objects are less impacted by partial volume effects and count statistics, the increased sensitivity in total-body PET offers greater improvements in detecting smaller lesions. This is reflected in our clinical routine, where we have had several examples of millimetric metastases that are unlikely to be seen on most conventional scanners (Figure 1) Moreover, choice of reconstruction parameters, such as point-spread function (PSF) modelling and iteration number, can be application-specific. Reconstructing images with no PSF modelling can result in higher image contrast and improved spatial resolution at lower iterations compared to reconstructions with PSF modelling, while PSF modelling converges to higher image contrast and improved spatial resolution at higher iterations. This is explained by slower initial convergence of the reconstruction with PSF modelling (Thielemans et al., 2010) and therefore, for lesion detection diagnostic tasks, PSF modelling allows for iterating longer to achieve higher contrast recovery at the same noise level.

Author Manuscript Author Manuscript Author Manuscript Author Manuscript

In addition to the improvements in image quality of normal-dose scans, total-body PET sensitivity has enabled ultra-low dose PET scans for the first time (Lan et al., 2021). NEMA image quality analysis results of the uEXPLORER using 18F-FDG has shown that the contrast recovery is not affected by reducing the scan duration or dose down to 30% of its original value, while image noise is minimally impacted (Spencer et al., 2021). Another concern about performing ultra-low-dose scans with total-body PET has been the higher flux of 176-Lu background radiation in total-body PET as a result of the large volume of LYSO crystals used in the scanner. Our current quantification study using phantom and human data suggests that quantification is minimally impacted when total 18F activity in the whole body varies from 17 MBq to 474 MBq, with mean biases in the range of ±5% (Leung et al., 2021). This confirms that effects from increased lutetium background and increased dead-time in total-body PET are both accounted for in data corrections and are not limiting factors in performing quantitative imaging with the uEXPLORER. Furthermore, our currently ongoing clinical studies with 90Y and 89Zr-labeled tracers have provided additional evidence on possibility of performing quantitative ultra-low-dose PET scans where only equivalent of 3.7 MBq of 18F are injected into the patients.

Finally, total-body PET offers unique opportunities and challenges in addressing one of the quantification barriers in PET, which is patient motion. Motion causes quantification bias by introducing image blurring and attenuation correction mismatch and it is a greater problem in total-body PET, as motion in one region of the body could affect the attenuation correction and scatter correction in other regions. As previously shown, high sensitivity of total-body PET allows sub-second dynamic frame reconstructions (Zhang et al., 2020). This enables the use of data-driven motion estimation techniques for obtaining either motion-free frames or reconstruction of motion corrected images.

2.1 Improved Image Quality

The improved spatial resolution and sensitivity of total-body scanners is best demonstrated by the substantial improvement in image quality that can be obtained compared to conventional scanners in the same acquisition time. The improved spatial resolution and sensitivity of total-body scanners needs to be considered during interpretation by trained radiologists, as even small findings may now show high uptake due to these improvements and may result in false positive calls.

Improved image quality also comes with logistical considerations. Large data sets are generated from the high counts gathered during each scan for reconstruction and can be used to generate high quality images with large matrix sizes; however, this leads to large image files, which may strain current PACS systems and storage capacity. Large data sets require longer processing and reconstruction times compared to conventional ones; this problem may improve in the near future thanks to advancements in reconstruction algorithms and computer hardware. Nevertheless, they are currently a considerable limitation. Interpretation of uEXPLORER images by radiologists at our institution can take up to 1.5 times longer than conventional scans, due to the increased number of images per scan, PACS issues (slow scrolling of images) and uncertainties that arise from higher detailed images. Even if images can be reconstructed with cuts smaller than 1 mm, in our clinical experience

Author Manuscript Author Manuscript Author Manuscript Author Manuscript

with the uEXPLORER, we typically reconstruct 2.33 mm slices as a compromise between image quality and logistic considerations (PACS and reading time). There remain gaps in knowledge regarding to what extent image quality improvement adds to clinical value beyond what is currently available, and such questions are being addressed in our current research.

2.2 Decreased Acquisition Time

The advancements in sensitivity and spatial resolution in total-body scanners can be used to decrease the overall acquisition time while maintaining diagnostic quality images. An example from the uEXPLORER can be seen in a lung cancer patient with acquisition times at 20, 10, 5 and 2.5 min (Figure 2), with all scans arguably considerable within diagnostic ranges, with varying degrees of noise. However, diagnostic quality of images from these short acquisition times may be below the quality of images from conventional clinical scanners, even if still able to provide with the necessary information to answer the clinical question. Before ordering scans with short acquisition time, the treating clinicians should be carefully counseled by the radiologist. A shorter acquisition time may be useful in improving image quality by reducing the extent of motion affecting the images, for example avoiding artefacts related to deep inspiration that is more likely to occur during a 20-minute scan compared to a 5-minute scan. Longer acquisition times produce images with lower noise, allowing for better detection and interpretation of scans (assuming image quality is not confounded by motion artifacts), while conversely patient comfort, patient access and financial considerations may encourage the use of shorter acquisition times.

Other clinical situations where there is increased need for reduced scan times include: pediatric population, in which anesthesia may possibly be avoided; high volume hospitals with limited scanner availability; and patients in considerable pain who are unable to tolerate long scans or cannot remain immobile. By surpassing the prior performance boundaries of conventional PET scanners, total-body scanners offer a choice to clinicians and radiologists in how to determine the optimal acquisition time for their clinical needs. At our institution, we have initially elected to prioritize image quality over most other considerations. This decision was carefully made and driven by a number of circumstances, including the fact that we were pioneers in the clinical total-body PET application and that our clinical practice was of moderate size, so that patient access pressure was not overwhelming. For imaging using ^{18}F-FDG and ^{68}Ga-DOTATATE, we currently use 20-minute scans, providing a good balance between very high image quality and motion artifacts. Of course, there is high variability in workflow and patient throughput times in different countries and institutions, and the optimal choice of acquisition time may therefore be different based on patient volumes, patient population, typical clinical practice and expectations, and other local considerations.

In addition to the most commonly used ^{18}F-FDG, also other FDA-approved radiotracers may benefit from decreased acquisition times, especially those in which small differences in acquisition time can greatly impacting biodistribution and interpretation of images. For example, the prostate cancer imaging tracer ^{18}F-Fluciclovine has shown to accumulate in prostate metastatic lesions with peak at 4–10 minutes post injection (Nanni et al., 2020). Due

Author Manuscript Author Manuscript Author Manuscript Author Manuscript

to limitations of conventional FOV scanners, EANM and SNMMI guidelines recommend scanning patients 3–5 min post injection, starting from the pelvic region/proximal thigh (with optimal dynamic scanning of this region at 0–5 min) and proceeding to the base of the skull (Nanni et al., 2020). Using this protocol in conventional scanners, the background uptake (especially in muscles) limits the evaluation of structures outside the pelvis (Calais et al., 2019). Taking into consideration the existing guidelines and the potential of the total-body scanner, we designed a clinical protocol that decreases the uptake in muscular structures, improving the quality of images, and that allows for reconstructing datasets that can help clarifying findings such as excreted activity in the bladder versus misregistered tumor recurrence in the prostatic bed. Our clinical protocol consists in the injection of 10 mCi of ^{18}F-Fluciclovine, followed by 24-minute dynamically acquired whole body scan with patients' arms up. The 3–6 minutes time frame is then reconstructed and used for interpretation. Other time points, before or after this time frame are used to clarify findings. For example, if there is focal radiotracer visualization in the prostate bed that can represent misregistered urine activity or vice-versa, we reconstruct time frames before kidney excretion occurs as visualized on the 3–6-minute reconstruction. If the 3-minute images are too noisy (for examples, due to patient body habitus), we reconstruct a larger dataset to distinguish between background noise and uptake. Ability to acquire good quality whole-body images in <5 min may increase detectability of lesions outside the prostate bed, potentially explaining or partially explaining the results of our recent work where ^{18}F-Fluciclovine had similar detection rate to PSMA (Azghadi et al., 2021).

2.3 Dose reduction

The quantity of administered radiotracer activity needed for optimal imaging is another factor of consideration in total-body PET scanners. The high signal collection efficiency of these scanners allows a significant decrease in the injected activity, thus reducing effective radiation dose to the patient. With the uEXPLORER PET/CT, both healthy and oncologic subjects have been shown to maintain diagnostic quality images even at low dose ranges with current low dose protocols(Ramsey D. Badawi et al., 2019). Examples of healthy subjects scanned with 14.8 MBq (0.4 mCi) and 74 (2 mCi) ^{18}F-FDG on EXPLORER PET/CT can be seen in (Figure 3) still showing diagnostic quality images (conventional doses for conventional PET/CT scanners are 370 MBq (10–20 mCi).

Dose reduction may provide clinical advantages in some circumstances; it can also improve staff safety and may help with logistical concerns for shorter lived radiotracers such as those labeled with ^{68}Ga such as ^{68}Ga-PSMA and ^{68}Ga-DOTATATE. Factors impacting the choice of activity to inject include the capacity of scanner to handle high (and low) count-rates, the radiosensitivity of the patient (discussed in more detail below), psycho-social concerns around radiophobia and the fact that reduced activity may require increased acquisition times to maintain image quality, bringing up considerations discussed in the previous section. In our practice, the standard dose used for ^{18}F-FDG EXPLORER PET/CT scans is 296 MBq (8 mCi) with an uptake time of 120 minutes.

Decrease in dose may be of great importance for several populations, such as for patients with radiation-sensitive syndromes (e.g., Fanconi syndrome, Li-Fraumeni syndrome), or

Author Manuscript Author Manuscript Author Manuscript Author Manuscript

pediatric population, given their higher sensitivity to radiation. While dose reduction will not particularly improve the risk profile of PET/CT imaging for typical adult oncologic patients, in some circumstances it may help reduce patient anxiety when discussing risks and benefits of the scan.

The capability of total-body PET scanners to provide diagnostic quality images with small amounts of activity in the field of view also opens new possibilities for the use of radioisotopes with poor dosimetry profiles that have had limited their use on conventional PET scanners until now. Long half-life positron emitting radioisotopes, in which the total amount of administered activity is restricted due to radiation safety, can facilitate the imaging of slow biological processes such as antibody uptake and clearance (Berg et al., 2020; Yoon et al., 2020). Examples include immuno-PET with isotopes such as ^{89}Zr, which has a physical half-life of 3.3 days. For ^{89}Zr the dose impact of the long half-life is compounded by the fact that its positron fraction is only ~20%, and effective dose per unit activity of ^{89}Zr-labeled antibodies can easily be 20–30 times greater than that for typical ^{18}F-labeled agents. Injected activities for these agents are therefore typically limited to ~75 MBq or less, resulting in very poor-quality images by conventional PET.

We have found that total-body PET overcomes these limitations, and we are currently using immuno-PET with various antibodies to study a wide range of diseases, from infectious diseases (Henrich et al., 2021) such as HIV and COVID-19 (Beckford Vera et al., 2020; Jones et al., 2021), to inflammatory conditions such as rheumatoid arthritis, and oncologic imaging. Henrich et al. and the University of California San Francisco team in their research with immuno-PET were able to successfully image HIV reservoirs by targeting CD4 binding sites of the HIV-1 external envelop protein using ^{89}Zr-labelled monoclonal antibodies in HIV positive patients (VanBrocklin et al., 2020) on the uEXPLORER PET/CT (Henrich et al., 2021). Total-body PET/CT may allow serial imaging up to 2–3 weeks, providing longitudinal tracking of CD4 cell populations (Henrich et al., 2021).

2.4 Delayed scanning

The ability to image patients with good diagnostic quality on total-body scanners with small amounts of activity in the field of view provides flexibility in the timing of image acquisition after dose administration. With high signal collection efficiency, total-body PET/CT scanners can extend and push the boundaries/limits of uptake time compared to conventional scanners. At our institution, IRB-approved protocols with healthy volunteers were used to compare image quality at varying time points. After the injection of 351.5 MBq (9.5 mCi) of ^{18}F-FDG, dynamic scans of 60 minutes and additional 20 min acquisition of static pictures at 60, 90 min, 3, 6, 9, and 12 hours were acquired (Figure 4). When the 60 min images are compared to 6-hour images, there is a decrease in blood pool and liver activity accompanied by an overall increase in noise level, however still within diagnostic quality compared to conventional PET. The group at the University of Pennsylvania using the PennPET EXPLORER (Karp et al., 2020) has had similar success with imaging ^{68}Ga-DOTATATE in a patient with metastatic neuroendocrine tumor up to 3.5 hours post-injection after the initial clinical scan at 65 min on a conventional scanner, with comparable diagnostic quality between scans (Pantel et al., 2020).

Author Manuscript Author Manuscript Author Manuscript Author Manuscript

The increased uptake time allows time for radiotracer clearance from certain regions of uptake such as blood pool and organs, potentially increasing the visibility of certain malignant processes, and reducing the visibility of inflammatory processes (Cheng et al., 2013; Hustinx et al., 1999). For diseases characterized by slow FDG uptake kinetics, such as epithelioid hemangioendothelioma (Dong et al., 2013), or for small lesions that may be hard to detect within high blood-pool background, this may render previously occult disease detectable.

Based on healthy volunteer cohort data and on literature (Cheng et al., 2013; Kubota et al., 2001) it has been shown that delayed imaging may help increase the detection of cancer by improved clearance in regions of significant background activity; this conclusion is consistent with our experience with our healthy volunteer cohort data. PennPET EXPLORER studies have demonstrated increased sensitivity in detection of perihepatic lesions and lymph nodes in a patient with metastatic colon cancer at delayed time points of 2.75 and 4.2 hours compared to 1.75 hours after injection (Pantel et al., 2020). Other radiotracers such as ^{68}Ga-PSMA have acceptable uptake time ranges of 50–100 min (Fendler et al., 2017), but have been shown to have increased lesion detection with delayed imaging up to 3–4 hours and can be used to clarify unclear lesions (Afshar-Oromieh et al., 2013).

Although delayed scanning appears advantageous, several challenges may arise. One of these include logistical issues, as routine clinical workflow protocols are based on conventional scanners. In our experience with the uEXPLORER PET/CT at UC Davis, we decided to extend the uptake time from 60 min to 2 hours based on discussions factoring the data from the healthy volunteer cohort, patient comfort, and logistics (number of technologists, injection rooms, etc.).

Another challenge that arises from delayed scanning is that longer uptake time introduces new interpretation questions for radiologists, as there is a substantial difference in blood pool and liver uptake at the 120 min time point compared to 60 min, due to increased clearance (Figure 5). The delayed uptake may help better detection of lesions and increase the radiologist confidence. However, increased clearance at longer time points may be misleading to radiologists when applying quantitative or semiquantitative clinical classifications such as Deauville/Lugano criteria/score (Cheson et al., 2014; Meignan et al., 2009) which are based on comparing lesion FDG avidity to blood pool and liver. These PET scoring systems are heavily used by oncologists and are based on the data available in the literature from conventional scanner studies. At the present time, there is insufficient data to convert these grading scores using a longer uptake time (120 min). Ongoing studies are currently being conducted at UC Davis to compare the differences in the 60 min vs 120 min time points to reevaluate the Deauville score in delayed imaging performed on total-body scanners in the prediction clinical outcome.

2.5 Simultaneous Total-Body Dynamic Imaging

Total-body PET enables simultaneous imaging of the entire body which can be used to provide high quality dynamic data covering all organs, tissues, and cells. This, in turn can be processed in a variety of ways including kinetic modeling and parametric imaging (X.

Author Manuscript Author Manuscript Author Manuscript Author Manuscript

Zhang et al., 2020), and analysis of multi-organ system relationships (Sundar et al., 2021) with potential uses in oncology, neurology, cardiology, and in those fields where the role of PET has not yet been well established due to conventional scanners' limitations, such as rheumatology, physiology and whole-person research. Total-body kinetic modeling allows for the creation of whole-body multiparametric images for values such as blood volume, blood flow, glucose metabolism, drug pharmacokinetics and pharmacodynamics (Wang et al., 2021).

While kinetic modeling and parametric imaging techniques for single organs have been well studied (Gallezot et al., 2020), total-body parametric imaging presents new challenges including tracer delivery delay and dispersion, variable mixtures of arterial and venous tracer supply, appropriate kinetic model selection for the different tissues in the body and motion correction. Work addressing all these issues is under way (Li et al., 2021; Sarkar et al., 2021; Shiyam Sundar et al., 2021; Wang et al., 2021; Zuo et al, 2018; Zuo et al., 2019).

The ability to visualize multiple parameters from the same scan not only provides new biomarkers but may also help with lesion detection in cancer, as imaging of glucose metabolic rate (ki) can improve lesion conspicuity in regions with high blood pool such as the liver, while imaging of glucose delivery (k1) may assist with detection in regions of high glucose metabolic rates (such as the brain) (Figure 6).

Depending on the tracer, clinical implementation of parametric imaging can be challenging due to the time required to track the relevant physiological processes. Fast processes such as FDG delivery can by mapped in a few minutes following injection (Feng et al., 2021), but glucose metabolic rate, for example, takes longer. Deep learning approaches to parametric imaging, combined with the high quality of the data afforded by total-body PET, may offer solutions to this dilemma in the future.

3. Conclusions

Total-body PET imaging at our institution has been demonstrated to provide many advantages over conventional PET imaging. Possible clinical applications provided by this technology include decreased overall acquisition time to as low as few minutes for improved throughput, patient motion mitigation and/or anesthesia avoidance, improved image quality for improved diagnostic accuracy, dose reduction to as low as 15 MBq (0.4 mCi) for improved safety and extension to new patient populations, increased delay of scan times post-injection for improved lesion detection, practical implementation of ^{89}Zr-antibody imaging for immunoPET, and simultaneous whole-body scanning for dynamic imaging of fast radiotracers such as ^{18}F-Fluciclovine and for parametric imaging. However, it comes with considerations for image quality *vs* acquisition time, challenges for adaptation of existing logistical workflows and clinical radiologic scoring interpretation. The increasing dissemination of total-body and long AFOV scanners worldwide requires further research for better understanding of their potentials and to allow for a smooth implementation of this technology in the radiology field.

Author Manuscript Author Manuscript Author Manuscript Author Manuscript

Acknowledgments

This paper has been supported by NIH R01CA249422-03.

We would like to thank the EXPLORER Molecular Imaging team including our Study Coordinators, Technologists and Scientists (in particular, Dr. Yasser Gaber Abdelhafez, Dr. Guobao Wang and Dr. Abhijit Chaudhari for figures) that have contributed to this work.

Abbreviations:

AFOV	axial field-of-view
FBP	forward-back-projection
FWHM	full width at half maximum
LORs	lines-of-response
LYSO	lutetium yttrium oxyorthosilicate
PSF	point-spread-function

References:

Afshar-Oromieh A et al. “Pet Imaging with a [68ga]Gallium-Labelled Psma Ligand for the Diagnosis of Prostate Cancer: Biodistribution in Humans and First Evaluation of Tumour Lesions.” European Journal of Nuclear Medicine and Molecular Imaging, vol. 40, no. 4, 2013, pp. 486–495, doi:10.1007/s00259-012-2298-2. [PubMed: 23179945]

Alberts Ian et al. “Clinical Performance of Long Axial Field of View Pet/Ct: A Head-to-Head Intra-Individual Comparison of the Biograph Vision Quadra with the Biograph Vision Pet/Ct.” European Journal of Nuclear Medicine and Molecular Imaging, vol. 48, no. 8, 2021, pp. 2395–2404, doi:10.1007/s00259-021-05282-7. [PubMed: 33797596]

Azghadi S et al. “Detectability Rates and Impact on Management from High-Sensitivity Total-Body 18f-Fluciclovine Pet/Ct Scans in Patients with Prostate Cancer Biochemical Recurrence.” International Journal of Radiation Oncology*Biology*Physics, vol. 111, no. 3, Supplement, 2021, pp. e264–e265, doi:10.1016/j.ijrobp.2021.07.867.

Badawi RD et al. “The Effect of Camera Geometry on Singles Flux, Scatter Fraction and Trues and Randoms Sensitivity for Cylindrical 3d Pet-a Simulation Study.” 1999 IEEE Nuclear Science Symposium. Conference Record. 1999 Nuclear Science Symposium and Medical Imaging Conference (Cat. No.99CH37019), IEEE. doi:10.1109/nssmic.1999.842848, 2021–10-01T01:56:18.

Badawi Ramsey D. et al. “First Human Imaging Studies with the Explorer Total-Body Pet Scanner*.” Journal of Nuclear Medicine, vol. 60, no. 3, 2019, pp. 299–303, doi:10.2967/jnumed.119.226498. [PubMed: 30733314]

Beckford Vera Denis et al. “First-in-Human Total-Body Pet Imaging of Hiv with ≪Sup≫89≪/Sup≫Zr-Vrc01 on the Explorer.” Journal of Nuclear Medicine, vol. 61, no. supplement 1, 2020, p. 545, http://jnm.snmjournals.org/content/61/supplement_1/545.abstract.

Berg E et al. “Total-Body Pet and Highly Stable Chelators Together Enable Meaningful (89)Zr-Antibody Pet Studies up to 30 Days after Injection.” J Nucl Med, vol. 61, no. 3, 2020, pp. 453–460, doi:10.2967/jnumed.119.230961. [PubMed: 31562219]

Calais J et al. “F-fluciclovine PET-CT and Ga-PSMA-11 PET-CT in patients with early biochemical recurrence after prostatetomy; a prospective, single-centre, single-arm, comparative imaging trial”. Lancet Oncol, vol. 20, no 9, 2019, pp1286–1294. [PubMed: 31375469]

Cheng Gang et al. “When Should We Recommend Use of Dual Time-Point and Delayed Time-Point Imaging Techniques in Fdg Pet?” European Journal of Nuclear Medicine and Molecular Imaging, vol. 40, no. 5, 2013, pp. 779–787, doi:10.1007/s00259-013-2343-9. [PubMed: 23361859]

Author Manuscript Author Manuscript Author Manuscript Author Manuscript

Cherry Simon R. “The 2006 Henry N. Wagner Lecture: Of Mice and Men (and Positrons)—Advances in Pet Imaging Technology.” Journal of Nuclear Medicine, vol. 47, no. 11, 2006, pp. 1735–1745. [PubMed: 17079804]

Cheson Bruce D. et al. “Recommendations for Initial Evaluation, Staging, and Response Assessment of Hodgkin and Non-Hodgkin Lymphoma: The Lugano Classification.” Journal of Clinical Oncology, vol. 32, no. 27, 2014, pp. 3059–3067, doi:10.1200/jco.2013.54.8800. [PubMed: 25113753]

Conti M et al. “Performance of a High Sensitivity Pet Scanner Based on Lso Panel Detectors.” IEEE Transactions on Nuclear Science, vol. 53, no. 3, 2006, pp. 1136–1142, doi:10.1109/tns.2006.875153.

Crosetto DB “The 3d Complete Body Screening (3d-Cbs) Features and Implementation.” 2003 IEEE Nuclear Science Symposium. Conference Record (IEEE Cat. No.03CH37515), IEEE. doi:10.1109/nssmic.2003.1352382, 2021-10-01T02:00:54.

Dong Aisheng et al. “Mri and Fdg Pet/Ct Findings of Hepatic Epithelioid Hemangioendothelioma.” Clinical nuclear medicine, vol. 38, no. 2, 2013, pp. e66–e73. [PubMed: 22996250]

Eriksson L et al. “An Investigation of Sensitivity Limits in Pet Scanners.” Nuclear Instruments and Methods in Physics Research Section A: Accelerators, Spectrometers, Detectors and Associated Equipment, vol. 580, no. 2, 2007, pp. 836–842.

Fendler Wolfgang P. et al. “68ga-Psma Pet/Ct: Joint Eanm and Snmmi Procedure Guideline for Prostate Cancer Imaging: Version 1.0.” European Journal of Nuclear Medicine and Molecular Imaging, vol. 44, no. 6, 2017, pp. 1014–1024, doi:10.1007/s00259-017-3670-z. [PubMed: 28283702]

Feng T et al. “Total-Body Quantitative Parametric Imaging of Early Kinetics of (18)F-Fdg.” J Nucl Med, vol. 62, no. 5, 2021, pp. 738–744, doi:10.2967/jnumed.119.238113. [PubMed: 32948679]

Gallezot JD et al. “Parametric Imaging with PET and SPECT” IEEE, vol 4, no. 1, 2020, pp 1–23

Henrich Timothy J et al. “Total-Body Pet Imaging in Infectious Diseases.” PET clinics, vol. 16, no. 1, 2021, pp. 89–97. [PubMed: 33160926]

Hustinx Roland et al. “Dual Time Point Fluorine-18 Fluorodeoxyglucose Positron Emission Tomography: A Potential Method to Differentiate Malignancy from Inflammation and Normal Tissue in the Head and Neck.” European Journal of Nuclear Medicine, vol. 26, no. 10, 1999, p. 1345, doi:10.1007/s002590050593. [PubMed: 10541835]

Jones Terry et al. “Total Body Pet Scanning of Cd8+ T-Lymphocytes to Study the Body’s Immune Defence System in Covid-19 Related Conditions.” Total bbody PET 2021, 2021.

Karp Joel S. et al. “Pennpet Explorer: Design and Preliminary Performance of a Whole-Body Imager.” Journal of Nuclear Medicine, vol. 61, no. 1, 2020, pp. 136–143, doi:10.2967/jnumed.119.229997. [PubMed: 31227573]

Kubota Kazuo et al. “Advantage of Delayed Whole-Body Fdg-Pet Imaging for Tumour Detection.” European Journal of Nuclear Medicine, vol. 28, no. 6, 2001, pp. 696–703, doi:10.1007/s002590100537. [PubMed: 11440029]

Lan Xiaoli et al. “Dynamic Pet Imaging with Ultra-Low-Activity of 18f-Fdg: Unleashing the Potential of Total-Body Pet.” European Journal of Nuclear Medicine and Molecular Imaging, 2021, doi:10.1007/s00259-021-05214-5.

Leung Edwin K et al. “Quantitative Accuracy in Total-Body Imaging Using the Uexplorer Pet/Ct Scanner.” Physics in Medicine & Biology, 2021.

Li EJ et al. “Efficient Delay Correction for Total-Body Pet Kinetic Modeling Using Pulse Timing Methods.” J Nucl Med, vol. In Press, 2021.

Meignan Michel et al. “Report on the First International Workshop on Interim-Pet Scan in Lymphoma.” Leukemia & Lymphoma, vol. 50, no. 8, 2009, pp. 1257–1260, doi:10.1080/10428190903040048. [PubMed: 19544140]

Nanni Cristina et al. “[18f]Fluciclovine Pet/Ct: Joint Eanm and Snmmi Procedure Guideline for Prostate Cancer Imaging—Version 1.0.” European Journal of Nuclear Medicine and Molecular Imaging, vol. 47, no. 3, 2020, pp. 579–591, doi:10.1007/s00259-019-04614-y. [PubMed: 31822959]

Author Manuscript Author Manuscript Author Manuscript Author Manuscript

Nardo Lorenzo et al. “Clinical Implementation of Total-Body Pet/Ct at University of California, Davis.” PET clinics, vol. 16, no. 1, 2021, pp. 1–7. [PubMed: 33218600]

Pantel Austin R. et al. “Pennpet Explorer: Human Imaging on a Whole-Body Imager.” Journal of Nuclear Medicine, vol. 61, no. 1, 2020, pp. 144–151, doi:10.2967/jnumed.119.231845. [PubMed: 31562224]

Sarkar S et al. “Dynamic Positron Emission Tomography/Computed Tomography Imaging Correlate of Nonalcoholic Steatohepatitis.” Clin Gastroenterol Hepatol, vol. 19, no. 11, 2021, pp. 2441–2443, doi:10.1016/j.cgh.2020.10.029. [PubMed: 33075553]

Sundar Shiyam, Lalith et al. “Data-Driven Motion Compensation Using Cgan for Total-Body [18f]Fdg-Pet Imaging.” Journal of Nuclear Medicine, vol. 62, no. supplement 1, 2021, p. 35, http://jnm.snmjournals.org/content/62/supplement_1/35.abstract.

Spencer Benjamin A. et al. “Performance Evaluation of the Uexplorer Total-Body Pet/Ct Scanner Based on Nema Nu 2–2018 with Additional Tests to Characterize Pet Scanners with a Long Axial Field of View.” Journal of Nuclear Medicine, vol. 62, no. 6, 2021, pp. 861–870, doi:10.2967/jnumed.120.250597. [PubMed: 33008932]

Sundar Lalith Kumar Shiyam et al. “Exploring Human Functional Connectome Using Total-Body Pet (Enhance-Pet). .” Total-Body PET 2021–2022 2021.

Thielemans K et al. “Impact of Psf Modelling on the Convergence Rate and Edge Behaviour of Em Images in Pet.” IEEE Nuclear Science Symposuim & Medical Imaging Conference, IEEE, 2010–10-01 2010. doi:10.1109/nssmic.2010.5874409, 2021–10-02T03:30:54.

VanBrocklin Henry et al. “Imaging Viral Load and T Cell Activation in Hiv: Tools for Cure Development.” Soc Nuclear Med, 2020.

Wang G et al. “Total-Body Pet Multiparametric Imaging of Cancer Using a Voxel-Wise Strategy of Compartmental Modeling.” J Nucl Med, 2021, doi:10.2967/jnumed.121.262668.

Watanabe M et al. “A High-Throughput Whole-Body Pet Scanner Using Flat Panel Ps-Pmts.” IEEE Transactions on Nuclear Science, vol. 51, no. 3, 2004, pp. 796–800, <Go to ISI>:// 000222644100030.

Wong Wai-Hoi et al. “The Initial Design and Feasibility Study of an Affordable High-Resolution 100-Cm Long Pet.” 2007 IEEE Nuclear Science Symposium Conference Record, IEEE, 2007–01-01 2007. doi:10.1109/nssmic.2007.4437029, 2021–10-01T02:03:06.

Yoon Joon-Kee et al. “Current Perspectives on 89zr-Pet Imaging.” International Journal of Molecular Sciences, vol. 21, no. 12, 2020, p. 4309, doi:10.3390/ijms21124309.

Zhang X et al. “Total-Body Dynamic Reconstruction and Parametric Imaging on the Uexplorer.” J Nucl Med, vol. 61, no. 2, 2020, pp. 285–291, doi:10.2967/jnumed.119.230565. [PubMed: 31302637]

Zhang Xuezhu et al. “Theoretical Study of the Benefit of Long Axial Field-of-View Pet on Region of Interest Quantification.” Physics in Medicine & Biology, vol. 63, no. 13, 2018, p. 135010, doi:10.1088/1361-6560/aac815. [PubMed: 29799814]

Zuo Y et al. “Relative Patlak Plot for Dynamic Pet Parametric Imaging without the Need for Early-Time Input Function.” Phys Med Biol, vol. 63, no. 16, 2018, p. 165004, doi:10.1088/1361-6560/aad444. [PubMed: 30020080]

Zuo Y et al. “Structural and Practical Identifiability of Dual-Input Kinetic Modeling in Dynamic Pet of Liver Inflammation.” Phys Med Biol, vol. 64, no. 17, 2019, p. 175023, doi:10.1088/1361-6560/ab1f29. [PubMed: 31051490]

Author Manuscript

Author Manuscript

Author Manuscript

Author Manuscript

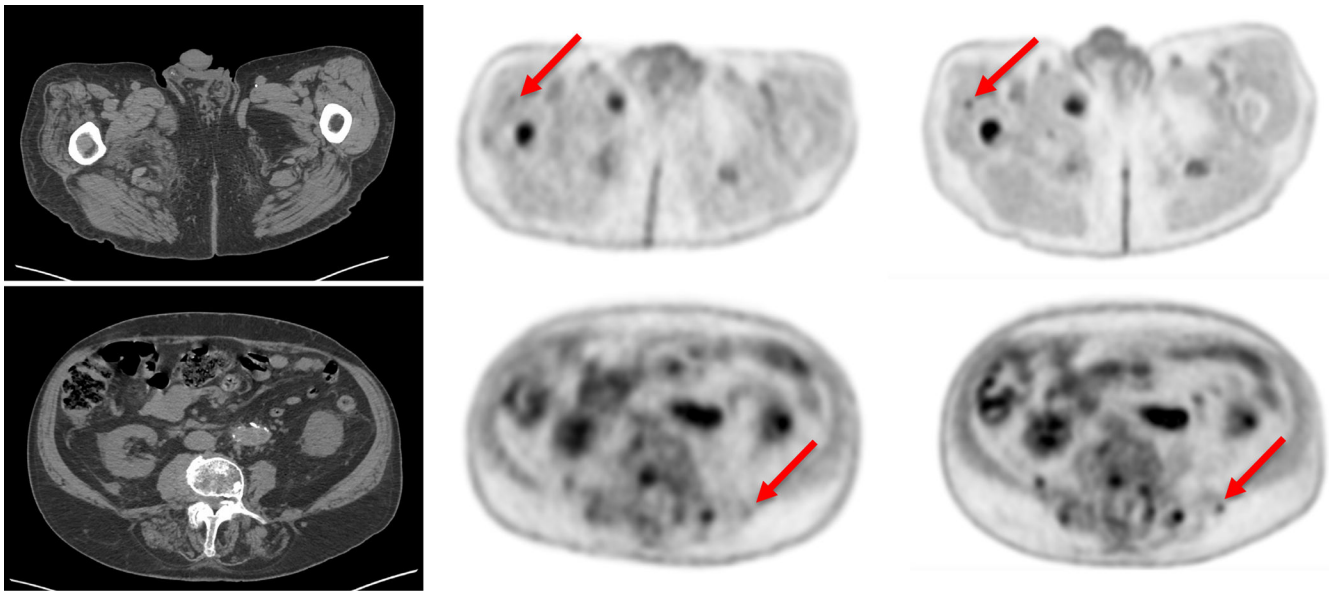

Figure 1.

Millimetric metastases (red arrows) in a Patient with stage IV lung cancer scanned on uExplorer (right column) and a conventional scanner (middle column) on the same day with ^{18}F-FDG. Note the higher level of detail provided by uEXPLORER images, given its increased sensitivity compared to conventional scanners.

Author Manuscript Author Manuscript Author Manuscript Author Manuscript

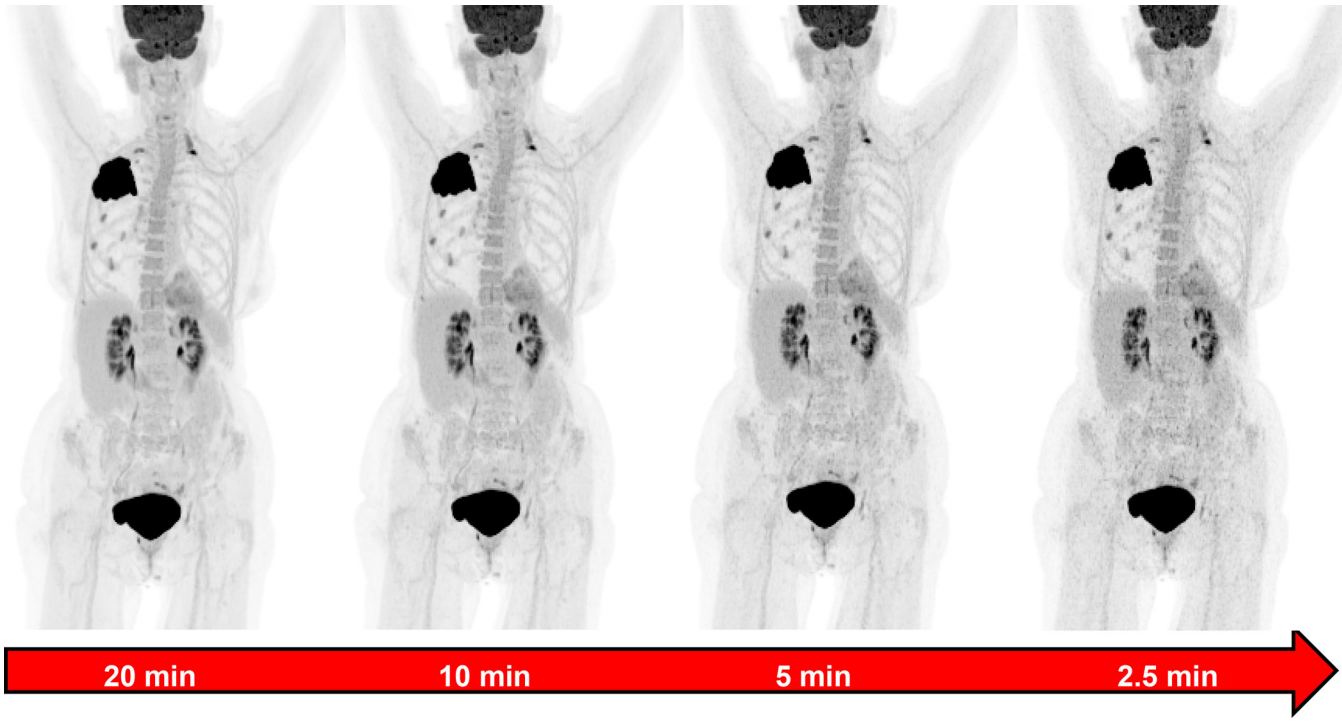

Figure 2.

Diagnostic quality images at reduced acquisition times in a patient with right upper lobe lung cancer. Image noise increases at shorter acquisition time; however, the quality of this scan at 2.5 minutes is still within the diagnostic range.

Author Manuscript Author Manuscript Author Manuscript Author Manuscript

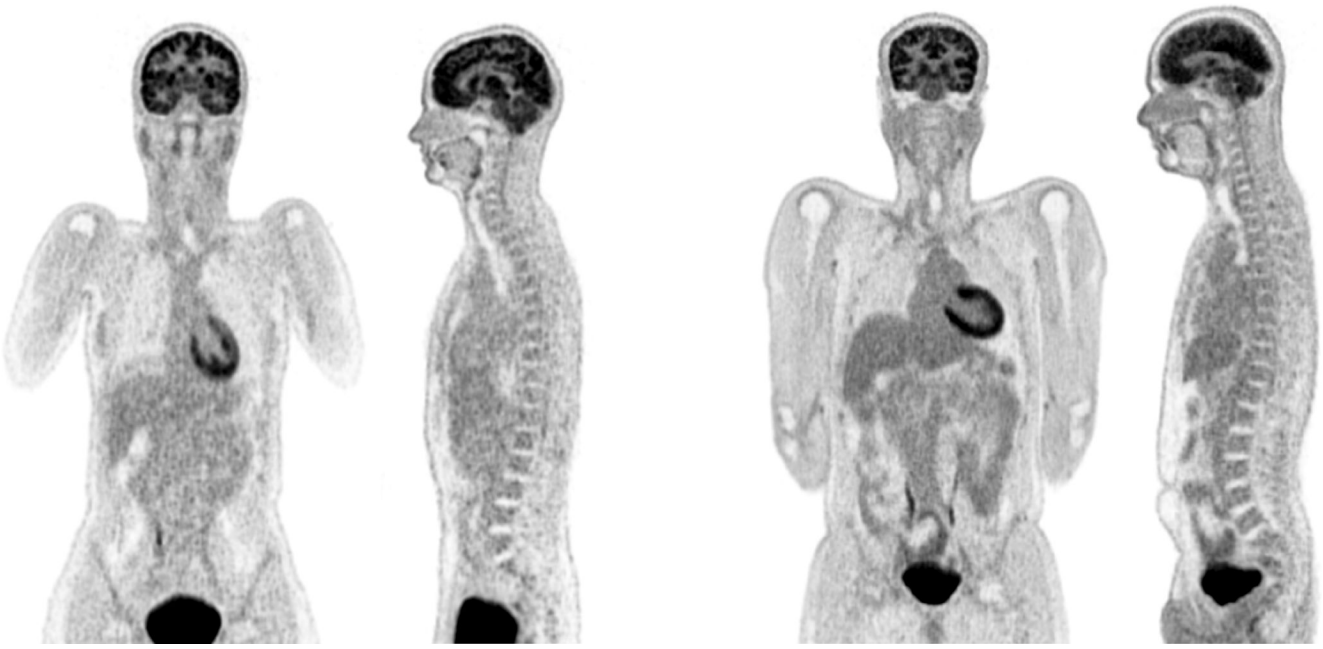

Figure 3.

Example of images from a healthy female volunteer scanned on the total-body scanner with 15 MBq (0,5 mCi, sagittal and coronal images on the left) and a healthy male subject scanned with 74 MBq (2mCi, sagittal and coronal images on the right) ^{18}F-FDG (courtesy of Dr. Chaudhari).

Author Manuscript Author Manuscript Author Manuscript Author Manuscript

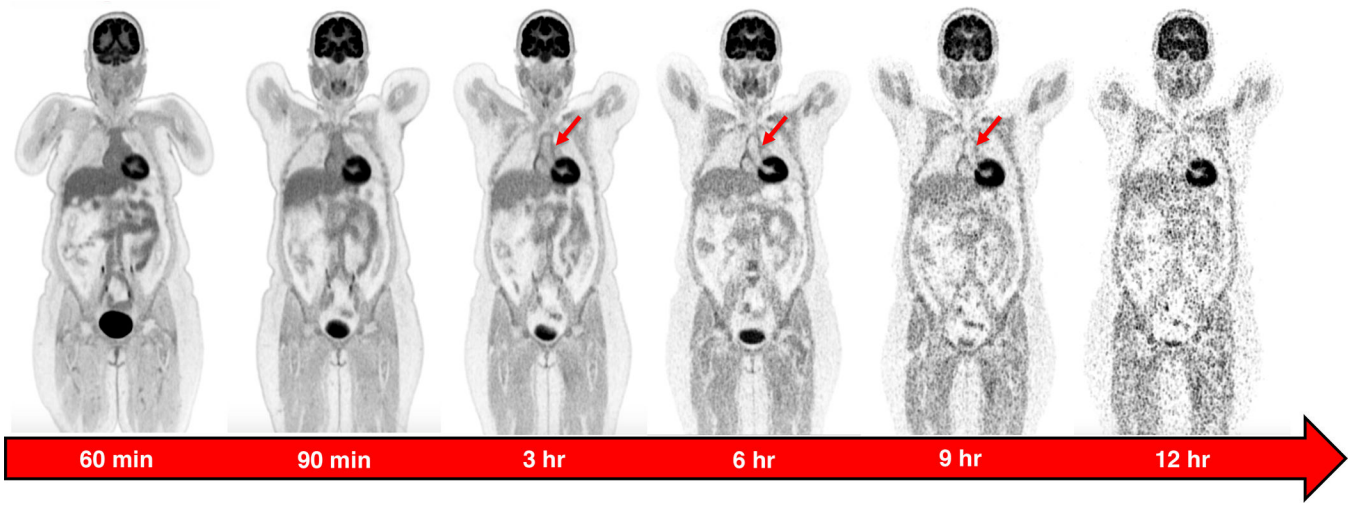

Figure 4.

Image quality comparison from a healthy female volunteer scanned on a total-body scanner at different uptake-times. Coronal cuts at the different time points demonstrate the change in biodistribution of FDG over time: note how the blood-pool clears over time (red arrows) leading to better visualization of vessel walls, while there is an overall increase in background noise. At 12 hours the image quality is below diagnostic range for several purposes.

Author Manuscript Author Manuscript Author Manuscript Author Manuscript

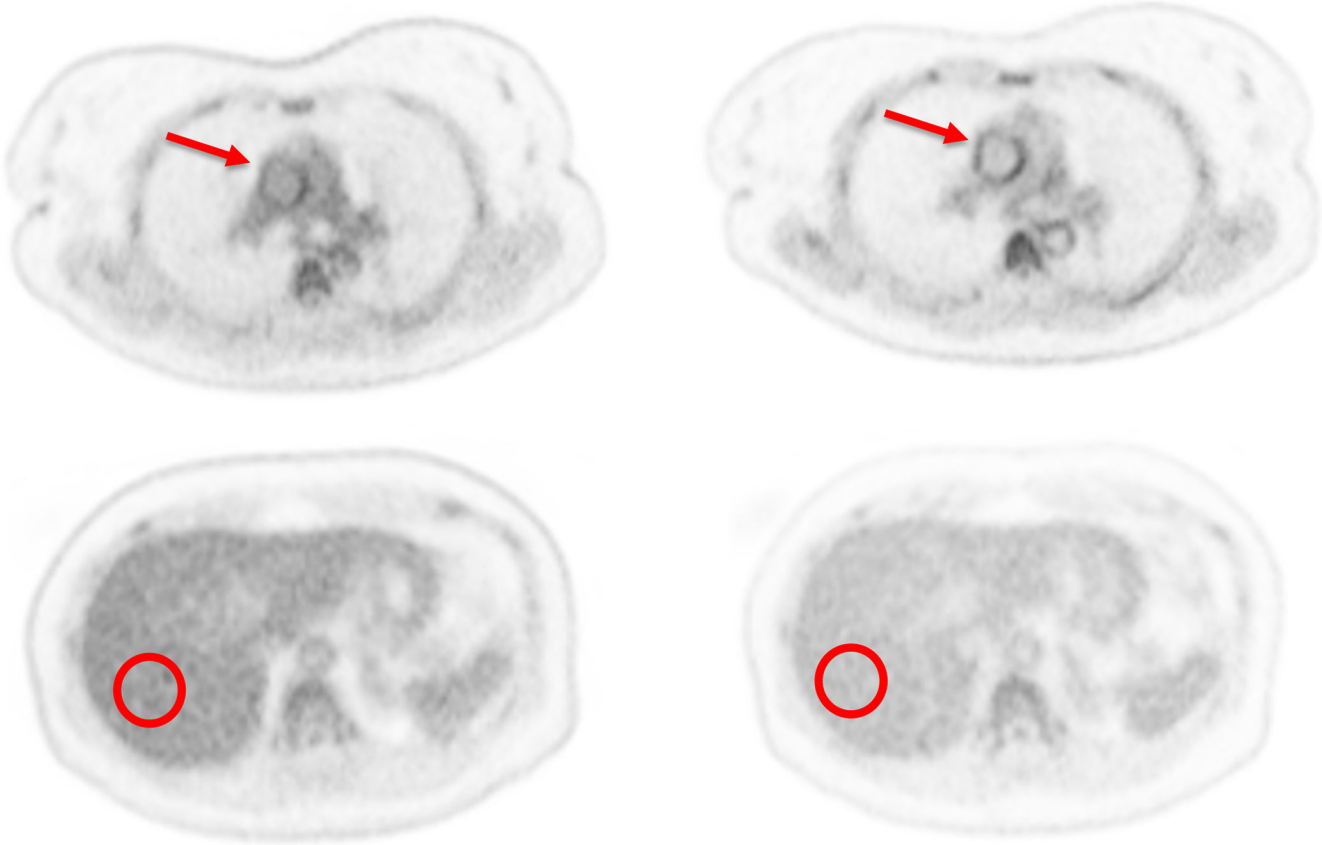

Figure 5.
uEXPLORER images of a patient with non-Hodgkin's lymphoma. Differences in blood pool (redarrows, upperrow) and liver uptake (red circles on the right haepatic lobe, lower row) at the 60 time-point (images on the left) compared to 120 min (images on the left), due to radiotracer clearance over time.

Author Manuscript

Author Manuscript

Author Manuscript

Author Manuscript

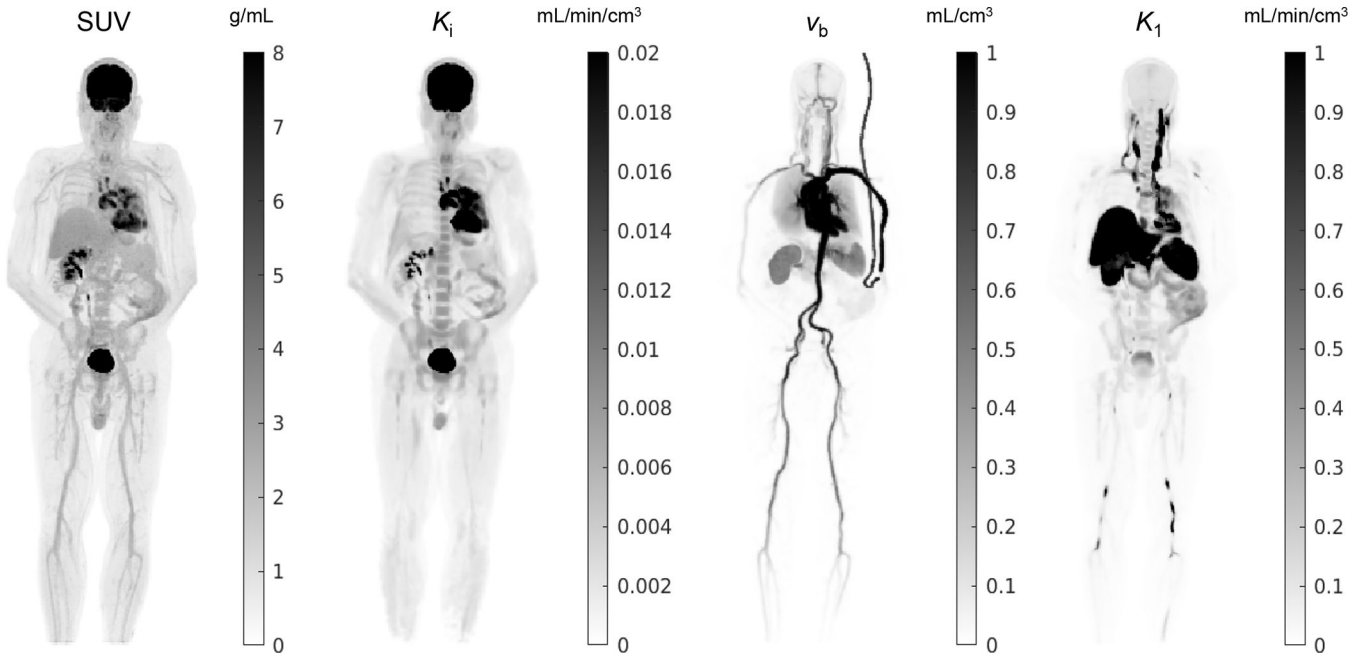

Figure 6.

Comparison of standard SUV image with parametric images of FDG influx rate K_i, fractional blood volume v_b, and FDG delivery rate K_1 of a cancer patient. Shown are maximum intensity projection maps (courtesy of Dr. Wang)